

Averting the Infrared Catastrophe in the Gold Standard of Quantum Chemistry

Nikolaos Masios, Andreas Irmiler, Tobias Schäfer, and Andreas Grüneis*

*Institute for Theoretical Physics, TU Wien,
Wiedner Hauptstraße 8-10/136, 1040 Vienna, Austria*

(Dated: March 1, 2024, PREPRINT)

Coupled-cluster theories can be used to compute *ab initio* electronic correlation energies of real materials with systematically improvable accuracy. However, the widely used coupled cluster singles and doubles plus perturbative triples [CCSD(T)] method is only applicable to insulating materials. For zero-gap materials the truncation of the underlying many-body perturbation expansion leads to an infrared catastrophe. Here, we present a novel perturbative triples formalism that yields convergent correlation energies in metallic systems. Furthermore, the computed correlation energies for the three-dimensional uniform electron gas at metallic densities are in good agreement with quantum Monte Carlo results. At the same time the newly proposed method retains all desirable properties of CCSD(T) such as its accuracy for insulating systems as well as its low computational cost compared to a full inclusion of the triples. This paves the way for *ab initio* calculations of real metals with chemical accuracy.

Introduction. — *Ab initio* methods that achieve systematically improvable accuracy for metallic systems are urgently needed to understand chemical reactions on metal surfaces or to compute the thermodynamic stability of materials. Currently available exchange and correlation energy density functionals often fail to achieve the desired level of accuracy compared to experiment. A prominent failure includes the incorrect prediction of molecular adsorption sites on metal surfaces [1]. As an alternative, more accurate quantum Monte Carlo (QMC) calculations can be applied to metals [2, 3]. However, even diffusion QMC calculations exhibit a strong dependence on the fixed node approximation [4]. Compared to QMC and density functional theory, many-electron perturbation theories offer a conceptually different approach to solve the many-electron problem with high accuracy. In particular, coupled-cluster (CC) theory offers a systematically improvable ansatz for the many-electron wave function employing a series of higher order particle-hole excitation operators. While systems exhibiting strong correlation, e.g. stretched covalent bonds, require high-order excitation operators or multireference approaches, single reference systems are already described accurately using low orders [5]. In particular, at the truncation level of single, double and perturbative triple particle-hole excitation operators, CCSD(T) theory predicts atomization and reaction energies for a wide class of single reference molecules with an accuracy of approximately 1 kcal/mol [5]. As such, CCSD(T) is often referred to as the “gold standard” of molecular quantum chemistry. This also motivated recent applications of coupled-cluster theory to study solids [6–11], where highly accurate predictions of, for example, pressure-temperature phase diagrams [12] could be achieved. However, it should be noted that such calculations require a careful convergence with respect to the employed basis sets and system size, which is much more complicated than for lower levels of theory [7, 10, 13].

Moreover, metallic systems still constitute a major challenge for currently available CC theories. Although CCSD can be applied to metals, recently obtained results for a number of metallic systems indicate that CCSD falls short of achieving chemical accuracy in metals, which is expected and agrees with findings for molecules and insulating solids [14, 15]. The inclusion of the perturbative triples correction (T) though, is not possible due to the infrared catastrophe caused by the truncation of the many-electron perturbation expansion [16]. The infrared catastrophe leads to a divergence of the CCSD(T) correlation energy per electron for metals for increasing simulation cell sizes also referred to as the thermodynamic limit (TDL). A full nonperturbative inclusion of the triple excitation operator in the CC method is convergent but computationally too expensive and can only be applied to few relatively small systems [17]. Here, we present a modification to the perturbative triples theory that is applicable to metals and retains all desirable properties including its accuracy for insulating systems and low computational cost compared to a full inclusion of the triples.

Theory. — To better understand the infrared catastrophe of perturbation theories denoted as (X), we make use of the following three quantities: the correlation energy $E_c^{(X)}$, the electronic transition structure factor $S^{(X)}(\mathbf{q})$ and the quantity $T_i^{(X)}(\mathbf{q})$. The correlation energy is defined as

$$E_c^{(X)} = \sum_{\mathbf{q}} v(\mathbf{q}) \underbrace{\left[\frac{\delta v_{ij}^{ab}}{\delta v(\mathbf{q})} (2t_{ij}^{ab} - t_{ji}^{ab}) \right]_{(X)}}_{:=S^{(X)}(\mathbf{q})}. \quad (1)$$

The indices i, j and a, b denote occupied and virtual spatial orbitals, respectively. Einstein summation convention applies to repeated indices throughout this work. We will first focus on second-order perturbation theory, direct ring CC doubles (rCCD) theory, which

is closely related to the random-phase approximation (RPA), and CC doubles theory (CCD). We note that, due to the symmetry of the uniform electron gas (UEG) Hamiltonian, single excitations are absent. Furthermore, in the UEG, the one-electron orbitals are plane waves with wave vectors \mathbf{k}_i , \mathbf{k}_j and \mathbf{k}_a , \mathbf{k}_b . This allows us to write the two-electron repulsion integral as $v_{ij}^{ab} = v(\mathbf{q})\delta_{\mathbf{k}_i-\mathbf{k}_a, \mathbf{k}_b-\mathbf{k}_j}$, with the momentum transfer vector $\mathbf{q} = \mathbf{k}_i - \mathbf{k}_a$, $v(\mathbf{q}) = \frac{4\pi}{\Omega|\mathbf{q}|^2}$ and Ω being the volume of the simulation cell. The functional derivative $\frac{\delta v_{ij}^{ab}}{\delta v(\mathbf{q})} = \delta_{\mathbf{q}, \mathbf{k}_b-\mathbf{k}_j} \delta_{\mathbf{q}, \mathbf{k}_i-\mathbf{k}_a}$ enables a concise notation. The amplitudes t_{ij}^{ab} are obtained by solving the amplitude equations of the employed many-electron perturbation theory.

Eq. (1) introduces the electronic transition structure factor $S(\mathbf{q})$, which gives access to the dependence of the correlation energy on the interelectronic interaction distance. An additional quantity of significance for the present work is given by

$$T_i^{(X)}(\mathbf{q}) = \left[\frac{\delta v_{ij}^{ab}}{\delta v(\mathbf{q})} t_{ij}^{ab(X)} \right]. \quad (2)$$

Similar to the structure factor, $T_i^{(X)}(\mathbf{q})$ depends on the momentum transfer vector \mathbf{q} .

The infrared catastrophe. — Having introduced the most important quantities needed for our analysis, we turn to the case of second-order perturbation theory, which is a textbook example for the infrared catastrophe. In particular, we focus on second-order Møller-Plesset perturbation theory (MP2), which employs the Hartree-Fock (HF) Hamiltonian as the unperturbed reference system [18].

The MP2 correlation energy is given by Eq. (1) using $t_{ij}^{ab} = v_{ij}^{ab}/\Delta_{ab}^{ij}$, where $\Delta_{ab}^{ij} = \varepsilon_i + \varepsilon_j - \varepsilon_a - \varepsilon_b$. The correlation energy for the UEG diverges due to the summation over elements in the amplitudes with both the occupied orbital i and the virtual orbital a close to the Fermi surface. The rate of divergence is $\log(q)$ [19] and $\log[\log(q)]$ [20] for Hartree or HF orbital energies, respectively. q refers to the lower spherical cutoff radius in the analytical integration over \mathbf{q} . Here, we employ HF orbital energies only. The comparison between analytic and numerical results is slightly complicated by the fact that Δ_{ab}^{ij} approaches the analytic behavior of $\lim_{\mathbf{q} \rightarrow 0} \Delta_{ab}^{ij} \propto |\mathbf{q}| \ln(|\mathbf{q}|)$ only slowly with respect to the studied system size. However, our numerical findings for t_{ij}^{ab} shown in Fig. 1(c) agree reasonably well with the analytic result of $\propto |\mathbf{q}|^{-3}/\log(|\mathbf{q}|)$. The infrared catastrophe due to the singularity of $S(\mathbf{q})$ at $|\mathbf{q}| = 0$ can be inferred from the plot for MP2 theory shown in Fig. 1(a).

The numerical procedure follows the description in Ref. [21]. We use twist averaging which helps to reduce the fluctuations due to discretization errors of the finite simulation cell [10, 22, 23].

The ring summation. — As already demonstrated by Macke in 1950 [24], the divergence in second-order perturbation theory can be averted by including carefully selected higher-order contributions of the many-electron perturbation expansion, corresponding to ring diagrams. Algebraically, this can be implemented by solving the ring-coupled-cluster amplitude equation given by

$$t_{ij}^{ab} = (v_{ij}^{ab} + 2v_{ic}^{ak} t_{kj}^{cb} + 2t_{ik}^{ac} v_{cj}^{kb} + 4t_{il}^{ad} v_{dc}^{lk} t_{kj}^{cb}) / \Delta_{ab}^{ij}, \quad (3)$$

which is formally equivalent to solving the Casida equations [25]. For the ring-coupled-cluster correlation energy to converge in the long wavelength limit, the first term on the right-hand side of Eq.(3), which is equivalent to MP2 theory, needs to be partially canceled by the additional linear ring (lr) and quadratic ring (qr) terms in the amplitudes.

We now address the question: How do the terms on the right-hand side in Eq. (3) cancel each other in the limit $|\mathbf{q}| \rightarrow 0$? To this end, we rewrite Eq. (3) in the following way

$$t_{ij}^{\text{rCCD}}(\mathbf{q}) = v(\mathbf{q}) \left(1 + 2 \sum_k t_{kj}^{\text{rCCD}}(\mathbf{q}) + 2 \sum_k t_{ik}^{\text{rCCD}}(\mathbf{q}) + 4 \sum_{kl} t_{il}^{\text{rCCD}}(\mathbf{q}) t_{kj}^{\text{rCCD}}(\mathbf{q}) \right) / \Delta_{ab}^{ij}, \quad (4)$$

which is possible because of momentum conservation and the fact that ring diagrams do not couple different \mathbf{q} . As was shown by Freeman in Ref. [26], the solution of the above equation in the long wave limit leads to $\lim_{\mathbf{q} \rightarrow 0} T_i^{\text{rCCD}}(\mathbf{q}) = -1/2$. Consequently, the terms in the parenthesis in Eq.(4) vanish such that $\lim_{\mathbf{q} \rightarrow 0} t_{ij}^{\text{rCCD}}(\mathbf{q}) \propto |\mathbf{q}|^{-1}$ [26]. We note that amplitudes diverging as $|\mathbf{q}|^{-1}$ yield convergent correlation energies and vanishing $S(\mathbf{q})$'s for small $|\mathbf{q}|$. The above findings are identical for Hartree and Hartree-Fock orbital energies. Fig. 1(c) depicts our numerical results for $t_{ij}^{\text{rCCD}}(\mathbf{q})$, which diverges with the analytically known behavior of $|\mathbf{q}|^{-1}$ in the long wavelength limit. See Supplemental Material, which includes Refs. [13, 27–35], for numerical results confirming that $\lim_{\mathbf{q} \rightarrow 0} T_i^{\text{rCCD}}(\mathbf{q}) = -1/2$.

We complement the above discussion by numerically studying the rCCD transition structure factor and its individual diagrammatic contributions [36] given by

$$S^{\text{rCCD}}(\mathbf{q}) = S^{\text{MP2}}(\mathbf{q}) + S^{\text{lr}}(\mathbf{q}) + S^{\text{qr}}(\mathbf{q}). \quad (5)$$

The calculated contributions to $S(\mathbf{q})$ are depicted in Fig. 1(a). Although the individual contributions diverge, the total rCCD transition structure factor converges towards zero in the limit of $\mathbf{q} \rightarrow 0$ [see Fig. 1(a)]. We arrive at the first important insight of this work. The singularity at $|\mathbf{q}| = 0$ in $S^{\text{MP2}}(\mathbf{q})$ is canceled by one-half of the linear ring terms, whereas the singularity of the quadratic

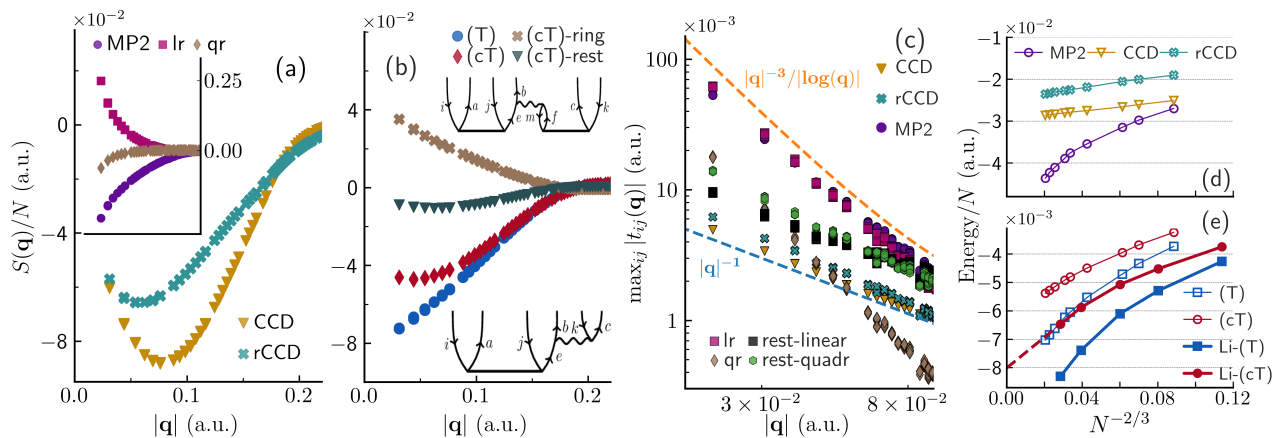


FIG. 1: (a) and (b) UEG transition structure factor contributions at different levels of theory for 246 electrons with 2178 spatial orbitals, 266 twists for rCCD, 166 twists for CCD, (T) and (cT) and $r_s = 20$ a.u. (c) Contributions to $t_{ij}(\mathbf{q})$ at different levels of theory for 730 electrons with 6254 spatial orbitals, 40 twists and $r_s = 20$ a.u. (d) and (e) CBS correlation energies per electron with 40 twists at $r_s = 3$ a.u. for the UEG retrieved as $N^{-2/3}$, where N is the electron number. (d) MP2, rCCD, and CCD correlation energies. (e) (T) and (cT) energies. (e) (T) and (cT) correlation energy per electron with 20 twists for Li denoted as Li-(T) and Li-(cT). Details in the Supplemental Material.

ring term is canceled by the “other” half of the linear term. We also stress that the leading-order behavior of $S^{\text{rCCD}}(\mathbf{q})$ in the limit $|\mathbf{q}| \rightarrow 0$ is $S^{\text{rCCD}}(\mathbf{q}) \propto |\mathbf{q}|$. This was shown by Bishop and Lührmann [37] (see Ref. [38] for a detailed discussion). For simulation cells with finite electron numbers this leads to a finite size error scaling of $N^{-2/3}$, where N is the number of electrons. Insulating systems have a different leading order behavior around $\mathbf{q} \rightarrow 0$ given by $S^{\text{rCCD}}(\mathbf{q}) \propto |\mathbf{q}|^2$, implying a finite size error scaling of N^{-1} [39, 40].

The coupled-cluster doubles method. – In addition to ring diagrams, CCD theory includes further terms, linear and quadratic in $t_{ij}^{\text{CCD}}(\mathbf{q})$ (the full set of CCD equations can be found in the Supplemental Material). This makes an analytic solution impossible even for the simple UEG model. Note that the contributions of the linear terms are even identical to those from third-order perturbation theory, if $t_{ij}^{\text{CCD}}(\mathbf{q})$ is replaced by $v_{ij}^{ab}/\Delta_{ab}^{ij}$. As discussed by Mattuk [19] for any finite-order perturbation theory, ring terms yield the most divergent contributions at small $|\mathbf{q}|$. We stress that the dominance of the ring terms originates from the “piling-up of factors $1/q^2$,” as the greatest piling-up occurs for the ring terms when only a single momentum transfer is involved [41]. Therefore, this dominance prevails irrespectively of the usage of $t_{ij}^{\text{CCD}}(\mathbf{q})$ instead of $v_{ij}^{ab}/\Delta_{ab}^{ij}$ at small $|\mathbf{q}|$. Consequently, it follows, in agreement with the work of Emrich and Zabolitzky [42], that for the long wavelength limit: (i) in the CCD amplitude equations the most divergent contributions are the ones given in Eq.(4), and (ii) these ring contributions to the CCD amplitudes must therefore cancel each other precisely as for the rCCD amplitude equations. This

leads us to one pivotal conclusion of the present work: $\lim_{|\mathbf{q}| \rightarrow 0} T_i^{\text{CCD}}(\mathbf{q}) = \lim_{|\mathbf{q}| \rightarrow 0} T_i^{\text{rCCD}}(\mathbf{q}) = -1/2$.

We corroborate the above paragraph with numerical results for the individual contributions to $t_{ij}^{\text{CCD}}(\mathbf{q})$. Fig. 1(c) depicts that the lr and qr contributions diverge as $\propto |\mathbf{q}|^{-3}/\log(q)$. Note that these lr and qr contributions are evaluated using CCD amplitudes. Moreover, it is shown that the remaining linear and quadratic contributions to the CCD amplitudes denoted as rest-linear and rest-quadr, respectively, diverge with a weaker power for $\mathbf{q} \rightarrow 0$. This underpins the conclusions drawn above that in the long wavelength limit: (i) the ring contributions to CCD amplitudes dominate, and (ii) the ring terms cancel each other precisely as in rCCD. Furthermore, we find that $t_{ij}^{\text{CCD}}(\mathbf{q}) \propto |\mathbf{q}|^{-1}$, which leads to a transition structure factor $S^{\text{CCD}}(\mathbf{q})$ depicted in Fig. 1(a) that approaches zero in the limit of $\mathbf{q} \rightarrow 0$.

Triple particle-hole excitation operators – We now turn to CC theories that approximate the triple particle-hole excitation operator in a perturbative manner. In these cases the post-CCSD correlation energy and transition structure factor contributions are given by

$$E_c^{(J)} = \sum_{\mathbf{q}} v(\mathbf{q}) \underbrace{\left[\frac{\delta W_{ijk}^{abc}}{\delta v(\mathbf{q})} (A_{abc}^{ijk})_{(J)} \right]}_{:=S^{(J)}(\mathbf{q})}. \quad (6)$$

Here, (J) refers to the employed approximation. In the case of (T), $A_{abc}^{ijk} = \bar{W}_{abc}^{ijk}/\Delta_{abc}^{ijk}$ with $\bar{X}_{abc}^{ijk} = \frac{4}{3}X_{abc}^{ijk} - 2X_{acb}^{ijk} + \frac{2}{3}X_{bca}^{ijk}$. Δ_{abc}^{ijk} refers to the difference in HF orbital energies for the occupied and unoccupied states labeled

by the respective indices. W_{ijk}^{abc} is defined as

$$W_{ijk}^{abc} = P_{ijk}^{abc} (t_{ij}^{ae} v_{ek}^{bc} - t_{im}^{ab} v_{jk}^{mc}). \quad (7)$$

The permutation operator P_{ijk}^{abc} is defined as $P_{ijk}^{abc} X_{ijk}^{abc} = X_{ijk}^{abc} + X_{ikj}^{acb} + X_{kij}^{cab} + X_{kji}^{cba} + X_{jki}^{bca} + X_{jik}^{bac}$. We employ the following functional derivative for a concise notation used to define the structure factor: $\frac{\delta W_{ijk}^{abc}}{\delta v(\mathbf{q})} = P_{ijk}^{abc} (t_{ij}^{ae} \delta_{\mathbf{q}, \mathbf{k}_k - \mathbf{k}_c} - t_{im}^{ab} \delta_{\mathbf{q}, \mathbf{k}_k - \mathbf{k}_c})$. Fig. 1(b) depicts $S^{(T)}(\mathbf{q})$, which shares many similarities with $S^{\text{MP2}}(\mathbf{q})$. Both $S(\mathbf{q})$'s exhibit a singularity for $|\mathbf{q}| \rightarrow 0$ and yield correlation energies per electron that diverge as the system size increases. The infrared catastrophe of (T) is caused by the unscreened Coulomb interactions included in the approximation to A_{abc}^{ijk} [16].

Here, we introduce a novel correlation energy expression that yields convergent energies for the UEG at the level of triple particle-hole excitation operators without depending on any ad hoc parameters. We refer to the method as (cT) because it includes the *complete* set of terms present in the triples amplitude equations in a non-iterative manner. Naturally, the coupling of triples amplitudes with each other is disregarded. Thus, in (cT) we use the following approximation to $A_{abc}^{ijk} = \bar{M}_{abc}^{ijk} / \Delta_{abc}^{ijk}$, where

$$M_{abc}^{ijk} = P_{ijk}^{abc} \left(t_{ij}^{ae} v_{ek}^{bc} + 2t_{ij}^{ae} v_{ef}^{bm} t_{mk}^{fc} + \dots \right). \quad (8)$$

For brevity we show only a selection of terms that exhibit a divergent behavior for $\mathbf{q} \rightarrow 0$. Note that the (T) and (cT) approximation to A_{abc}^{ijk} agrees for all terms linear in t_{ij}^{ab} . To cancel the divergence in (T), (cT) includes additional ring terms such as the second term in the above equation. We show the diagrams corresponding to both terms from Eq. (8) in Fig. 1(b). For these terms, it follows that $v_{ek}^{bc} + 2v_{ef}^{bm} t_{mk}^{fc} = v_{ek}^{bc} [1 + 2T_m(\mathbf{q}')]$, with $\mathbf{q}' = \mathbf{k}_k - \mathbf{k}_c$. Note that $\mathbf{q}' \rightarrow 0 : 1 + 2T_m(\mathbf{q}') = 0$, which is formally identical to our results for the cancellation of the divergence between the linear ring and the MP2 terms in the long wavelength limit. We stress that (cT) also includes additional *rest* terms that are not related to the divergence of (T). The complete expression of M_{abc}^{ijk} including all contributions can be found in the Supplemental Material and Ref. [43].

As supporting numerical evidence, Fig. 1(b) depicts $S^{(cT)}(\mathbf{q})$, which exhibits a qualitatively different behavior than $S^{(T)}(\mathbf{q})$ and indicates convergence in the long wavelength limit. Furthermore, $S^{(cT)\text{-ring}}(\mathbf{q})$ is shown to cancel the divergence of $S^{(T)}(\mathbf{q})$. For completeness, Fig. 1(b) also depicts $S^{(cT)\text{-rest}}(\mathbf{q})$, which includes all contributions to Eq. (8) that are not included in (T) or (cT)-ring, e.g., exchange-like terms. Our findings show that $S^{(cT)\text{-rest}}(\mathbf{q})$ converges to zero as $\mathbf{q} \rightarrow 0$. This shows that the (cT) correlation energy expression averts the infrared catastrophe of the (T) approximation for the UEG

without requiring an iterative solution of the triple amplitudes as recently proposed in Ref. [44].

Results. — We now turn to the discussion of numerical results for correlation energies obtained for electron gas simulation cells with various electron numbers at different levels of theory. Fig. 1(d-e) display the behavior of the correlation energy per electron as a function of $N^{-2/3}$ for MP2, rCCD, CCD, (T) and (cT). The employed system sizes vary from $N = 38$ electrons to 342 electrons. All presented correlation energies have been extrapolated to the complete basis set (CBS) limit. The infrared catastrophe in MP2 theory becomes visible on approach to the TDL ($N \rightarrow \infty$) for Fig. 1(d). In contrast, rCCD and CCD correlation energies deviate considerably from the MP2 counterpart, converging as $N^{-2/3}$ to the TDL. In an analogous way, Fig. 1(e) verifies that the (T) correlation energy contribution also diverges as we move to the TDL, while its counterpart, (cT), exhibits a behavior that more closely resembles that of rCCD and CCD theories.

Table I summarizes correlation energies obtained from CCD, CCD(T), and CCD(cT) methods compared to i-FCIQMC, DMC, and CCDT (CCD with full triple excitations) results. The energies were extrapolated to the CBS limit, and the systems were parametrized by a range of Wigner-Seitz radii ($r_s = 1, 2, 3, 5, 10$ a.u.) and $N = 14, 54$ electrons. We first discuss the results obtained for the 14 electron system. In this case i-FCIQMC can be viewed as an exact reference, whereas CCDT serves as a reference for any approximate triples theory. CCDT results from Ref. [17] are in good agreement with i-FCIQMC in the high density limit and differ at low densities. Higher levels of CC theory are needed to capture all important correlation effects for increasing r_s [17]. CCD(T) and CCD(cT) correlation estimates are in good agreement with CCDT. We note that the agreement between CCD(T) and CCDT is fortuitous and only valid for small N , as can be seen from the divergence of CCD(T) as a function of N in Fig. 1(e).

We now discuss the results obtained for the 54 electron system summarized in Table I. Here, we compare to DMC reference results. In this case CCD(T) is fortuitously close to DMC even at relatively low densities corresponding to $r_s = 10$ a.u. As can be seen from Fig. 1(b) and Fig. 1(e), this agreement is due to error cancellation between two effects. On the one hand, (T) overestimates long range correlation effects. On the other hand, higher-order cluster operators are missing in CCD(T), which underestimates correlation effects at lower densities. This error cancellation fails for larger electron numbers. CCD(cT) averts the infrared catastrophe and obtains accurate correlation energy results compared to DMC for all densities up to $r_s = 5$ a.u. Only at lower densities CCD(cT) starts to deviate significantly from DMC due to the neglect of higher-order cluster operators.

TABLE I: CBS limit correlation energies per electron of the UEG in mHa. r_s is given in atomic units.

Method	14 electrons				54 electrons			
	$r_s = 1$	$r_s = 2$	$r_s = 3$	$r_s = 5$	$r_s = 1$	$r_s = 2$	$r_s = 5$	$r_s = 10$
CCD	-36.7	-29.2	-24.2	-18.1	-38.4	-30.2	-18.5	-11.3
CCD(T)	-37.9	-31.5	-27.1	-21.4	-39.9	-33.1	-22.6	-15.0
CCD(cT)	-37.8	-31.3	-26.9	-21.1	-39.8	-32.8	-22.1	-14.5
CCDT ^a	-37.9	-31.5	-27.0	-21.2				
i-FCIQMC ^b	-38.0	-31.8	—	-21.9				
DMC ^c					-39.0	-32.6	-22.8	-15.6

^a CCDT data are from the work of Neufeld and Thom [17].

^b i-FCIQMC data are from the work of Shepherd *et al.* [45]

^c These DMC data are from the work of López Ríos *et al.* [46]

As an important test, we apply CCSD(cT) theory to a set of molecules. In our benchmark we use a set of 26 different molecules that give access to 23 different closed-shell reaction energies. This selection of molecules was already used in a previous work [13]. As reference we use energies from a converged CCSDT calculation. The standard deviation of the reaction energy for the 23 reactions is 0.9 kJ/mol for both CCSD(T) and CCSD(cT) [the maximum error is 2.1 and 3.3 kJ/mol for CCSD(T) and CCSD(cT), respectively]. This illustrates that both, -CCSD(T) and CCSD(cT), are very accurate approximations for the full CCSDT energy.

Finally, we present results for the lithium bcc metal. We find that CCSD(cT) predicts a cohesive energy of 60.1 mHa/atom in excellent agreement with the experimental estimate of 60.9 mHa/atom corrected for zero-point vibrations [47]. Our estimate includes a HF, CCSD, (cT) and core-valence MP2 contribution of 20.5, 30.4, 8, and 1.2 mHa/atom, respectively. The computational details are discussed in the Supplemental Material. Fig. 1(e) depicts the (cT) correlation energy convergence. Although our CCSD estimate of the cohesion energy is in good agreement with results from Ref. [44], we note that our triples estimate is about 3 mHa/atom larger.

Summary and conclusions. — We have introduced the highly accurate and computationally efficient CCSD(cT) theory, which paves the way for achieving chemical accuracy in *ab initio* calculations of real metals. Although the presented approach was applied to paramagnetic systems only, it can also be generalized to ferromagnetic systems using an unrestricted formalism. Several far reaching conclusions must be drawn from the present work. The RPA in the electron gas is formally identical to CCSD in the long wavelength limit. Therefore embedding CCSD into the RPA should also be a promising approach for metals [48, 49]. Furthermore our work could explain (part of) the discrepancies observed between DMC and CCSD(T) interaction energies of large molecules [50].

The authors thankfully acknowledge support and funding from the European Research Council (ERC) under the European Union’s Horizon 2020 research and innovation program (Grant Agreement No. 715594). We

gratefully acknowledge many fruitful discussions with Felix Hummel, Alejandro Gallo, and James Shepherd. The computational results presented have been achieved in part using the Vienna Scientific Cluster (VSC).

* andreas.gruneis@tuwien.ac.at

- [1] P. J. Feibelman, B. Hammer, J. K. Nørskov, F. Wagner, M. Scheffler, R. Stumpf, R. Watwe, and J. Dumesic, *The Journal of Physical Chemistry B* **105**, 4018 (2001).
- [2] M. Pozzo and D. Alfè, *Phys. Rev. B* **78**, 245313 (2008).
- [3] K. Doblhoff-Dier, J. Meyer, P. E. Hoggan, and G.-J. Kroes, *Journal of Chemical Theory and Computation* **13**, 3208 (2017), pMID: 28514594, <https://doi.org/10.1021/acs.jctc.7b00344>.
- [4] N. Nemeč, M. D. Towler, and R. J. Needs, *The Journal of Chemical Physics* **132**, 034111 (2010), <https://doi.org/10.1063/1.3288054>.
- [5] R. J. Bartlett and M. Musiał, *Rev. Mod. Phys.* **79**, 291 (2007).
- [6] G. H. Booth, A. Grüneis, G. Kresse, and A. Alavi, *Nature* **493**, 365 (2013).
- [7] J. McClain, Q. Sun, G. K.-L. Chan, and T. C. Berkelbach, *J. Chem. Theory Comput.* **13**, 1209 (2017), arXiv:1701.04832.
- [8] J. Yang, W. Hu, D. Usvyat, D. Matthews, M. Schütz, and G. K.-L. Chan, *Science* **345**, 640 (2014).
- [9] A. Grüneis, *The Journal of Chemical Physics* **143**, 102817 (2015), <https://doi.org/10.1063/1.4928645>.
- [10] T. Gruber, K. Liao, T. Tsatsoulis, F. Hummel, and A. Grüneis, *Phys. Rev. X* **8**, 021043 (2018).
- [11] L. Weiler, T. N. Mihm, and J. J. Shepherd, *The Journal of Chemical Physics* **156** (2022), 10.1063/5.0086580, 204109.
- [12] T. Gruber and A. Grüneis, *Phys. Rev. B* **98**, 134108 (2018).
- [13] A. Irmeler, A. Gallo, and A. Grüneis, *The Journal of Chemical Physics* **154**, 234103 (2021), <https://doi.org/10.1063/5.0050054>.
- [14] T. N. Mihm, T. Schäfer, S. K. Ramadugu, L. Weiler, A. Grüneis, and J. J. Shepherd, *Nature Computational Science* **1**, 801 (2021).
- [15] V. A. Neufeld, H.-Z. Ye, and T. C. Berkelbach, *The Journal of Physical Chemistry Letters* **13**, 7497 (2022), pMID: 35939802, <https://doi.org/10.1021/acs.jpcclett.2c01828>.
- [16] J. J. Shepherd and A. Grüneis, *Phys. Rev. Lett.* **110**, 226401 (2013).
- [17] V. A. Neufeld and A. J. W. Thom, *The Journal of Chemical Physics* **147**, 194105 (2017), <https://doi.org/10.1063/1.5003794>.
- [18] C. Møller and M. S. Plesset, *Phys. Rev.* **46**, 618 (1934).
- [19] R. D. Mattuck, *A guide to Feynman diagrams in the many-body problem*, 2nd ed., Dover books on physics and chemistry (Dover Publications, New York, 1992).
- [20] F. E. Harris, H. J. H. J. Monkhorst, and D. L. Freeman, *Algebraic and diagrammatic methods in many-fermion theory* (1992) pp. vii + 403.
- [21] J. J. Shepherd, T. M. Henderson, and G. E. Scuseria, *J. Chem. Phys.* **140**, 124102 (2014).
- [22] N. D. Drummond, R. J. Needs, A. Sorouri, and W. M. C. Foulkes, *Phys. Rev. B* **78**, 125106 (2008).

- [23] C. Lin, F. H. Zong, and D. M. Ceperley, *Phys. Rev. E* **64**, 016702 (2001).
- [24] W. Macke, *Z. Naturforsch.* **5a**, 192 (1950).
- [25] G. E. Scuseria, T. M. Henderson, and D. C. Sorensen, *J. Chem. Phys.* **129**, 231101 (2008).
- [26] D. L. Freeman, *Phys. Rev. B* **15**, 5512 (1977).
- [27] G. Knizia, T. B. Adler, and H.-J. Werner, *The Journal of Chemical Physics* **130**, 054104 (2009), <https://doi.org/10.1063/1.3054300>.
- [28] M. Valiev, E. Bylaska, N. Govind, K. Kowalski, T. Straatsma, H. Van Dam, D. Wang, J. Nieplocha, E. Apra, T. Windus, and W. de Jong, *Comput. Phys. Commun.* **181**, 1477 (2010).
- [29] “cc4s; available from <https://manuals.cc4s.org>.” .
- [30] A. Gallo, F. Hummel, A. Irmmler, and A. Grüneis, *J. Chem. Phys.* **154**, 064106 (2021).
- [31] S. Hirata, I. Grabowski, M. Tobita, and R. J. Bartlett, *Chemical Physics Letters* **345**, 475 (2001).
- [32] G. Kresse and J. Furthmüller, *Phys. Rev. B* **54**, 11169 (1996).
- [33] G. Kresse and D. Joubert, *Phys. Rev. B* **59**, 1758 (1999).
- [34] A. Grüneis, G. H. Booth, M. Marsman, J. Spencer, A. Alavi, and G. Kresse, *J. Chem. Theory Comput.* **7**, 2780 (2011).
- [35] F. Hummel, T. Tsatsoulis, and A. Grüneis, *J. Chem. Phys.* **146**, 124105 (2017).
- [36] A. Irmmler, A. Gallo, F. Hummel, and A. Grüneis, *Phys. Rev. Lett.* **123**, 156401 (2019).
- [37] R. F. Bishop and K. H. Lührmann, *Phys. Rev. B* **26**, 5523 (1982).
- [38] T. N. Mihm, L. Weiler, and J. J. Shepherd, *Journal of Chemical Theory and Computation* **0**, null (2023), pMID: 36918372, <https://doi.org/10.1021/acs.jctc.2c00737>.
- [39] K. Liao and A. Grüneis, *J. Chem. Phys.* **145**, 141102 (2016).
- [40] R. Martin, L. Reining, and D. Ceperley, *Interacting Electrons* (Cambridge University Press, 2016).
- [41] M. Gell-Mann and K. A. Brueckner, *Phys. Rev.* **106**, 364 (1957).
- [42] K. Emrich and J. G. Zabolitzky, *Phys. Rev. B* **30**, 2049 (1984).
- [43] P. Piecuch, S. A. Kucharski, K. Kowalski, and M. Musiał, *Computer Physics Communications* **149**, 71 (2002).
- [44] V. A. Neufeld and T. C. Berkelbach, (2023), [arXiv:2303.11270](https://arxiv.org/abs/2303.11270) [cond-mat.mtrl-sci].
- [45] J. J. Shepherd, A. Grüneis, G. H. Booth, G. Kresse, and A. Alavi, *Phys. Rev. B* **86**, 035111 (2012).
- [46] P. López Ríos, A. Ma, N. D. Drummond, M. D. Towler, and R. J. Needs, *Phys. Rev. E* **74**, 066701 (2006).
- [47] L. Schimka, J. Harl, and G. Kresse, *The Journal of Chemical Physics* **134** (2011), [10.1063/1.3524336](https://doi.org/10.1063/1.3524336), 024116.
- [48] T. Schäfer, F. Libisch, G. Kresse, and A. Grüneis, *The Journal of Chemical Physics* **154**, 011101 (2021), <https://doi.org/10.1063/5.0036363>.
- [49] T. Schäfer, A. Gallo, A. Irmmler, F. Hummel, and A. Grüneis, *The Journal of Chemical Physics* **155**, 244103 (2021), <https://doi.org/10.1063/5.0074936>.
- [50] Y. S. Al-Hamdani, P. R. Nagy, A. Zen, D. Barton, M. Kállay, J. G. Brandenburg, and A. Tkatchenko, *Nature Communications* **12**, 3927 (2021).

Supplemental Material for: Averting the infrared catastrophe in the gold standard of quantum chemistry

Nikolaos Masios, Andreas Irmeler, Tobias Schäfer, and Andreas Grüneis*
*Institute for Theoretical Physics, TU Wien,
Wiedner Hauptstraße 8-10/136, 1040 Vienna, Austria*

NUMERICAL RESULTS FOR $T_i(\mathbf{q})$

In the main article the behaviour for the quantity $T_i(\mathbf{q})$ is discussed for values $\mathbf{q} \rightarrow 0$. In Fig. 1 we show numerical results for the UEG obtained with rCCD and CCD. One can see that minimum value of $T_i(\mathbf{q})$ converges slowly to the theoretical expected limit of -0.5. For rCCD results with larger electron numbers are presented below.

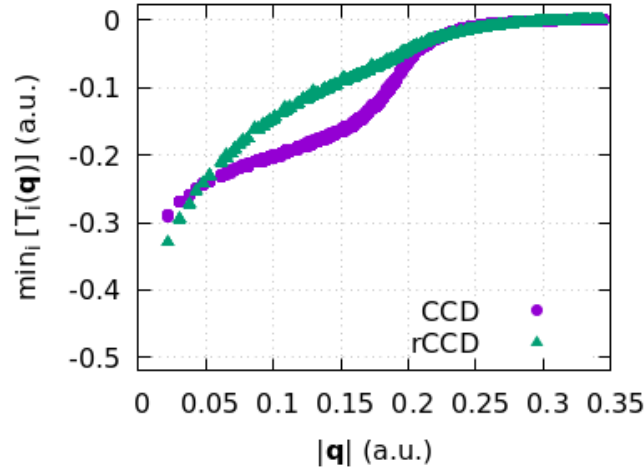


FIG. 1. The minimum value for a given momentum transfer \mathbf{q} is shown for the quantity $T_i(\mathbf{q})$. Results are shown for rCCD and CCD. Both simulations employed 730 electrons and a density of $r_s = 20$.

STRUCTURE FACTOR FOR DIFFERENT VALUES OF r_s

The discussion in the main article was based on a structure factor obtained for a density of $r_s = 20$. Fig. 2 shows structure factors for different values of r_s . This illustrates that the discussed behaviour of the structure factor not only holds for $r_s = 20$, but is also true for the important range of values between 1 and 5. However, for larger values of r_s the minimum of the structure factor is already observable for smaller electron numbers. This was the reason for choosing a rather high value of r_s in the main article. In both calculations, roughly 18 virtual spatial orbitals per occupied spatial orbital are used.

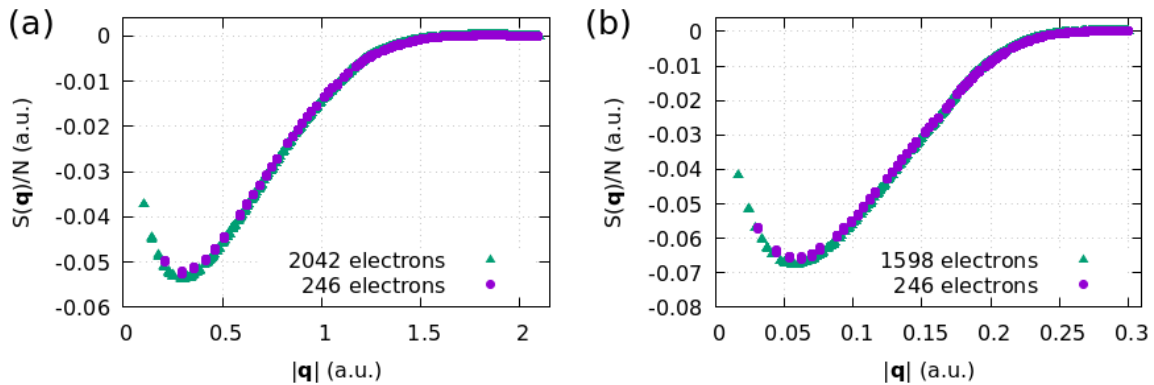


FIG. 2. For two different number of electrons N , twist-averaged structure factors for rCCD are shown. (a) shows results for $r_s = 3$, (b) shows results for $r_s = 20$.

arXiv:2303.16957v4 [cond-mat.mtrl-sci] 29 Feb 2024

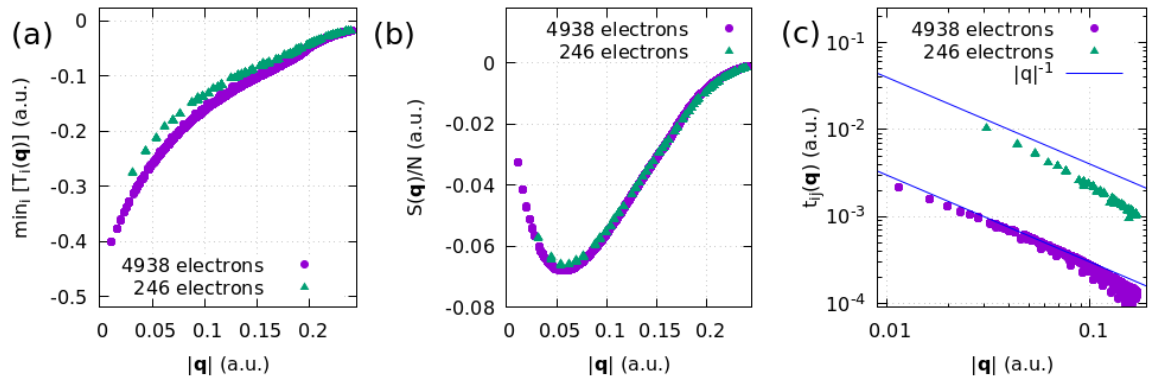


FIG. 3. Results obtained using a Hartree–Fock reference for two different electron numbers N and a density of $r_s = 20$. (a) shows $\min_i [T_i(\mathbf{q})]$, whereas (b) shows $S(\mathbf{q})$ as defined in the main article. (c) shows the largest t -amplitude element with a given momentum transfer \mathbf{q} .

RCCD RESULTS FOR LARGER ELECTRON NUMBERS

Figure 3 shows rCCD results using $N = 4938$ electrons together with data for $N = 246$ electrons. Similar to the numerical results in the main article, a Hartree–Fock reference is used in this calculations. Fig. 3(a) shows a very slow convergence of $\min_i [T_i(\mathbf{q})] \rightarrow -0.5$ for $\mathbf{q} \rightarrow 0$, whereas (b) shows the structure factor for both electron numbers. Finally, Fig. 3(c) shows the largest t -amplitude element on an absolute scale for a given \mathbf{q} -point. It can be seen that the theoretical expected $1/|\mathbf{q}|$ divergence for small values of \mathbf{q} sets in only for very large electron numbers. This is a consequence of the finite size error. In all calculations, roughly 18 virtual spatial orbitals per occupied spatial orbital are used.

TABLE I. Triple particle-hole excitation correlation energy contributions calculated with an aug-cc-pVTZ basis set. (T) and (cT) are computed using a one-shot approach as described in the main article. The energy for the full T, given in the last column, is evaluated by $E_T = E(CCSDT) - E(CCSD)$. All energies in atomic units.

Molecule	(T)	(cT)	T
C2H2	-0.01709	-0.01575	-0.01709
C2H4	-0.01550	-0.01440	-0.01588
CH3Cl	-0.01657	-0.01537	-0.01728
CH3OH	-0.01587	-0.01471	-0.01613
CH3SH	-0.01663	-0.01547	-0.01745
CH4	-0.00653	-0.00616	-0.00693
CO	-0.01789	-0.01642	-0.01800
CO2	-0.03031	-0.02769	-0.03001
CS2	-0.03663	-0.03330	-0.03702
Cl2	-0.01952	-0.01802	-0.02046
ClF	-0.01867	-0.01727	-0.01924
F2	-0.01966	-0.01818	-0.01967
H2	0.00000	0.00000	0.00000
H2O	-0.00867	-0.00805	-0.00874
H2O2	-0.02022	-0.01861	-0.02018
H2S	-0.00867	-0.00814	-0.00941
HCHO	-0.01757	-0.01620	-0.01771
HCN	-0.01889	-0.01732	-0.01867
HCOOH	-0.02799	-0.02569	-0.02795
HCl	-0.00876	-0.00816	-0.00933
HF	-0.00755	-0.00702	-0.00758
HNCO	-0.03044	-0.02783	-0.03027
N2	-0.01981	-0.01810	-0.01944
N2H4	-0.01760	-0.01627	-0.01776
NH3	-0.00833	-0.00777	-0.00854
SO2	-0.03679	-0.03346	-0.03645

MOLECULAR TESTSET

Table I summarizes correlation energy contributions obtained using different triple particle-hole excitation approximations. The geometries can be found in the work of Knizia et al. [1]. For these calculations the Hartree-Fock ground state was obtained with the NWChem package [2] and interfaced to cc4s [3] as described in Ref. [4]. The here employed testset was already used in a previous work [5]. This is where Hartree-Fock and CCSD energies for the given molecules can be found.

COUPLED CLUSTER DOUBLES (CCD) AMPLITUDE EQUATION

Here we present the closed-shell coupled-cluster doubles amplitude equations, which can also be found elsewhere[6]. The first line contains all contributions of the rCCD method. The second line contains all further terms which are linear in t_{ij}^{ab} , denoted as rest-linear in the main article. The other terms are further quadratic contributions to the CCD amplitude equation, denoted as rest-quadr in the main article.

$$\Delta_{ij}^{ab} t_{ij}^{ab} = v_{ij}^{ab} + P \sum_{kc} 2v_{ic}^{ak} t_{kj}^{cb} + P \sum_{kcl d} 2t_{il}^{ad} v_{dc}^{lk} t_{kj}^{cb} \quad (1)$$

$$+ \sum_{kl} v_{ij}^{kl} t_{kl}^{ab} + \sum_{cd} v_{ab}^{cd} t_{ij}^{cd} - P \sum_{kc} v_{ci}^{ak} t_{kj}^{cb} - P \sum_{kc} v_{ic}^{ak} t_{kj}^{bc} - P \sum_{kc} v_{ci}^{bk} t_{kj}^{ac} \quad (2)$$

$$+ \sum_{kcl d} t_{kl}^{ab} v_{cd}^{kl} t_{ij}^{cd} - P \sum_{ckld} 2t_{ij}^{cb} v_{cd}^{kl} t_{kl}^{ad} + P \sum_{ckld} t_{ij}^{cb} v_{dc}^{kl} t_{kl}^{ad} - P \sum_{kcl d} 2t_{kj}^{ab} v_{cd}^{kl} t_{il}^{cd} + P \sum_{kcl d} t_{kj}^{ab} v_{dc}^{kl} t_{il}^{cd} \quad (3)$$

$$+ P \sum_{kcl d} \frac{1}{2} t_{il}^{da} v_{cd}^{lk} t_{kj}^{cb} + P \sum_{kcl d} \frac{1}{2} t_{il}^{db} v_{cd}^{lk} t_{kj}^{ac} - P \sum_{kcl d} t_{il}^{da} v_{dc}^{lk} t_{kj}^{cb} \quad (4)$$

$$+ P \sum_{kcl d} \frac{1}{2} t_{il}^{da} v_{dc}^{lk} t_{kj}^{bc} - P \sum_{kcl d} t_{il}^{ad} v_{dc}^{lk} t_{kj}^{bc} - P \sum_{kcl d} t_{il}^{ad} v_{cd}^{lk} t_{kj}^{cb} + P \sum_{kcl d} \frac{1}{2} t_{il}^{ad} v_{cd}^{lk} t_{kj}^{bc} \quad (5)$$

$$P\{\dots\}_{ij}^{ab} = \{\dots\}_{ij}^{ab} + \{\dots\}_{ji}^{ba} \quad (6)$$

PERTURBATIVE TRIPLE PARTICLE-HOLE EXCITATION METHODS

In this section we present the full (cT) equations complementing Eq. (8) in the main article. In addition we present the equations for (T), (cT)-ring, (cT)-rest as they are used in the article. The following equation is used for all employed methods

$$M_{abc}^{ijk} = P_{ijk}^{abc} \left(\sum_e t_{ij}^{ae} J_{ek}^{(X)bc} - \sum_m t_{im}^{ab} J_{jk}^{(X)mc} \right), \quad (7)$$

with different definitions for $J^{(X)}$ for $X \in (\text{T}), (\text{cT}), (\text{cT})\text{-ring}, (\text{cT})\text{-rest}$ as defined below. We note that $J^{(\text{cT})\text{-rest}}$ is defined implicitly via

$$J^{(\text{T})} + J^{(\text{cT})\text{-ring}} + J^{(\text{cT})\text{-rest}} = J^{(\text{cT})} \quad (8)$$

The (T) method

In the (T) method the following intermediates are used

$$J_{ek}^{bc} = v_{ek}^{bc}, \quad (9)$$

$$J_{jk}^{mc} = v_{jk}^{mc} \quad (10)$$

The (cT)-ring term

For the (cT)-ring terms, the following intermediates are used

$$J_{ek}^{bc} = \sum_{mf} 2v_{ef}^{bm} t_{km}^{cf}, \quad (11)$$

$$J_{jk}^{mc} = \sum_{nf} 2v_{jf}^{mn} t_{kn}^{cf} \quad (12)$$

The (cT) method

In the (cT) method the following intermediates are used

$$J_{ek}^{bc} = v_{ek}^{bc} + \sum_f v_{ef}^{ab} t_k^f - \sum_m (\chi_{ke}^{mb} t_m^c + t_m^b \chi_{ek}^{mc} + I_e^m t_{mk}^{bc}) + \sum_{mf} \left(2\chi_{ef}^{bm} t_{km}^{cf} - \chi_{ef}^{bm} t_{km}^{fc} - \chi_{fe}^{bm} t_{mk}^{fc} - t_{km}^{fb} \chi_{fe}^{cm} \right) + \sum_{mn} t_{mn}^{cb} \chi_{ke}^{mn}, \quad (13)$$

$$J_{jk}^{mc} = v_{jk}^{mc} - \sum_n v_{jk}^{mn} t_n^c + \sum_f \left(\chi_{jf}^{mc} t_k^f + t_j^f \chi_{fk}^{mc} \right) + \sum_{nf} \left(2\chi_{jf}^{mn} t_{kn}^{cf} - \chi_{jf}^{mn} t_{kn}^{fc} - \chi_{jf}^{nm} t_{nk}^{fc} - t_{nj}^{cf} \chi_{kf}^{nm} \right) + \sum_{ef} t_{kj}^{ef} \chi_{ef}^{cm}, \quad (14)$$

$$\chi_{ke}^{mb} = v_{ke}^{mb} - \frac{1}{2} \sum_n v_{ke}^{mn} t_n^b + \sum_f t_k^f \chi_{ef}^{bm}, \quad (15)$$

$$\chi_{ef}^{bm} = v_{ef}^{bm} - \frac{1}{2} \sum_n t_n^b v_{ef}^{nm}, \quad (16)$$

$$\chi_{ek}^{mc} = v_{ek}^{mc} - \frac{1}{2} \sum_n v_{ek}^{mn} t_n^c + \sum_f \chi_{fe}^{cm} t_k^f, \quad (17)$$

$$I_c^m = f_c^m + \sum_{nf} (2v_{cf}^{mn} t_n^f - v_{fc}^{mn} t_n^f), \quad (18)$$

$$\chi_{ef}^{bm} = \chi_{ef}^{bm} - \frac{1}{2} \sum_n t_n^b v_{ef}^{nm}, \quad (19)$$

$$\chi_{ke}^{mn} = v_{ke}^{mn} + \sum_f t_k^f v_{fe}^{mn}, \quad (20)$$

$$\chi_{jf}^{mc} = v_{jf}^{mc} - \sum_n v_{jf}^{mn} t_n^c + \frac{1}{2} \sum_g t_j^g \chi_{fg}^{cm}, \quad (21)$$

$$\chi_{fk}^{mc} = v_{fk}^{mc} - \sum_n v_{fk}^{mn} t_n^c + \frac{1}{2} \sum_g \chi_{gf}^{cm} t_k^g, \quad (22)$$

COMPUTATIONAL DETAILS ON THE CALCULATIONS OF METALLIC LITHIUM

Metallic body-centered cubic (BCC) lithium is considered. All calculations are performed using the Vienna Ab initio Simulation Package (VASP) [7] for HF and MP2 energies, as well as *cc4s* code [3] for coupled cluster energies. VASP is based on periodic boundary conditions and makes use of the projector augmented-wave (PAW) formalism [8]. We consider one valence electron per Li atom, using the PAW POTCAR file labeled as `Li_GW` and a plane-wave cutoff parameter of `ENCUT = 141 eV`.

For efficient coupled cluster calculations, a compression of the unoccupied HF manifold is achieved via approximate MP2 natural orbitals (NOs) [9], while a low-rank decomposition is employed to compress the Coulomb integrals as described in Ref. [10]. Both schemes introduce a controllable error which is kept well below 10^{-2} mHa for the low-rank decomposition of the Coulomb integrals. The basis-set error of the CCSD correlation contribution, as introduced by the restricted number of NOs, is converged to sub-mHa accuracy using a recently proposed focal-point correction scheme (here denoted as FPC) [5], as can be observed in Fig. 5(b). For the (cT) and (T) correlation contribution, a relatively small number of 5 NOs per occupied orbital is used and corrected by an $1/N_{NO}$ extrapolation from 5 to 10 NOs using a simulation cell containing 26 Li atoms. This is sufficient, since the basis-set dependence of both (cT) and (T) is weak.

Furthermore, the core-valence contribution to the correlation energy is estimated by an all-electron PAW POTCAR file labeled as `Li_AE_GW`. In this case three electrons per Li atom are considered as valence electrons. Since the $1s^2$ HF orbitals are located about -63 eV below the Fermi level, we consider the MP2 method as sufficient for this task. Here a plane-wave cutoff of `ENCUT = 543 eV` is used. The individual contributions to the atomization energy of bulk bcc lithium are reported in the main document.

THERMODYNAMIC LIMIT EXTRAPOLATION

Fig 5(a)+(c) depicts the thermodynamic limit extrapolation of the HF and CCSD correlation energies of bulk bcc lithium. The corresponding numerical data is summarized in Tab.II. We find that using the extrapolation law of $(N_k N_{\text{atoms}})^{-2/3}$ fits the computed energies and enables a precise extrapolation. Here N_k denotes the number of k-points used to sample the first Brillouin zone. We note that Brillouin zone sampling with more than one k-point is not yet supported in *cc4s*. Therefore all post-HF calculations employ $N_k = 1$ and large supercells with geometries given below. However, twist-averaging is used to reduce the fluctuations due to discretization errors of the finite simulation cells. The geometries and atomic structures of these cells are given below. The employed power law for the extrapolation to the limit $N \rightarrow \infty$ is well justified by the linear behaviour of the CCSD structure factor in the long wave length limit $\mathbf{q} \rightarrow 0$. However, this also implies that the system sizes included in such an extrapolation have to be large enough to sample sufficiently short wavevectors in reciprocal space where the structure factor approaches $\mathbf{q} \rightarrow 0$ linearly.

The extrapolation of the (cT) correlation energy contribution for lithium shown in the main article, employs an $(N_{\text{atoms}})^{-2/3}$ fit and system sizes of 128 and 208 atoms. We note, however, that the (cT) correlation energies obtained for smaller systems deviate from the employed extrapolation law. To estimate the remaining uncertainty in the thermodynamic limit extrapolation of the (cT) energy we have performed the following analysis based on the UEG.

Fig. 4 depicts the (cT) correlation energies of the UEG for a range of electron numbers at a density corresponding to $r_s=3.2$. This density and the employed basis set sizes are identical to the calculations for lithium. Our findings indicate that the difference between thermodynamic limit extrapolations employing the $(N)^{-2/3}$ fits and system sizes corresponding to 358-610 electrons and 128-208 electrons deviate by less than 0.5 mHa/electron. Furthermore the extrapolated estimates using 358-610 electrons and 208-358 electrons correspond to -5.2 mHa/electron and -5.3 mHa/electron, deviating by less than 0.1 mHa/electron. From this we estimate that the remaining uncertainty in our estimate of the (cT) contribution to the lithium cohesive energy obtained from extrapolations using 128 and 208 atoms is below 1 mHa/atom. Tab. III summarizes the numerical data of (cT) energies for the UEG and lithium.

$N_k N_{\text{atoms}}$	HF	$N_k N_{\text{atoms}}$	CCSDc
216	-0.08344	26	-0.02463
343	-0.08280	44	-0.02633
512	-0.08237	68	-0.02727
729	-0.08210	128	-0.02841

TABLE II. Total energies of the plots (a) and (c) of Fig. 5 of this Supplemental Material. The energies are in Ha per atom.

N_{elect}	UEG-(cT)	Li-(cT)
26	-1.60	-3.75
44	-2.15	-4.52
68	-2.72	-5.07
128	-3.37	-5.88
208	-3.76	-6.47
358	-4.20	—
610	-4.53	—

TABLE III. Tabulated correlation contribution at the level of (cT) to the atomization energy of Li as depicted in Fig. 1 of the main manuscript. UEG-(cT) energies are discussed in the text. All energies in mHa per electron.

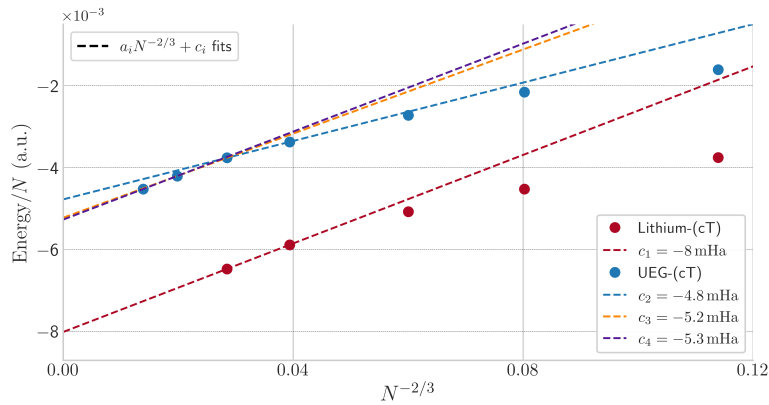


FIG. 4. Thermodynamic limit convergence of the (cT) energy per electron.

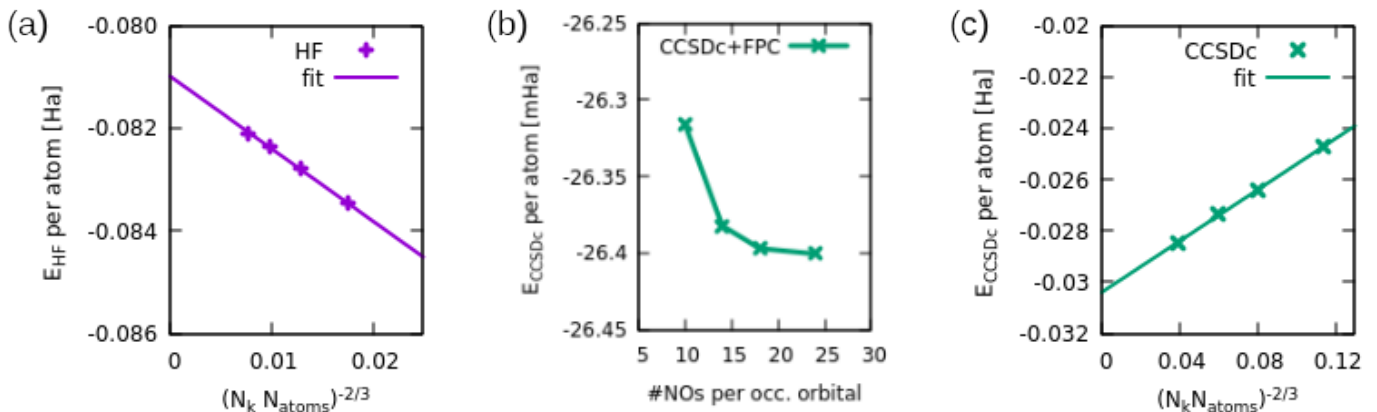


FIG. 5. (a) Thermodynamic limit convergence of the HF energy per atom. (b) Basis-set convergence of the CCSD correlation energy per atom using a simulation cell with 44 Li atoms. (c) Thermodynamic limit convergence of the CCSD correlation energy per atom.

Atomic structures of the used bcc lithium supercells in units of Ångstrom.

26 atoms

volume of cell : 535.2100

lattice vectors of the cell

```
6.905952995 -3.452976497 3.452976497
0.000000000 6.905952995 3.452976497
-3.452976497 -3.452976497 6.905952995
```

length of vectors

```
8.458030512 7.721090173 8.458030512
```

position of ions in fractional coordinates

```
0.000000000 0.000000000 0.000000000
0.923076923 0.384615385 0.846153846
0.615384615 0.923076923 0.230769231
0.461538462 0.692307692 0.923076923
0.846153846 0.769230769 0.692307692
0.153846154 0.230769231 0.307692308
0.538461538 0.307692308 0.076923077
0.230769231 0.846153846 0.461538462
0.384615385 0.076923077 0.769230769
0.769230769 0.153846154 0.538461538
0.076923077 0.615384615 0.153846154
0.307692308 0.461538462 0.615384615
0.692307692 0.538461538 0.384615385
0.230769231 0.346153846 0.961538462
0.153846154 0.730769231 0.807692308
0.846153846 0.269230769 0.192307692
0.692307692 0.038461538 0.884615385
0.076923077 0.115384615 0.653846154
0.384615385 0.576923077 0.269230769
0.769230769 0.653846154 0.038461538
0.461538462 0.192307692 0.423076923
0.615384615 0.423076923 0.730769231
0.000000000 0.500000000 0.500000000
0.307692308 0.961538462 0.115384615
0.538461538 0.807692308 0.576923077
0.923076923 0.884615385 0.346153846
```

44 atoms

volume of cell : 905.7400

lattice vectors of the cell

```
3.452976497 -6.905952995 6.905952995
0.000000000 6.905952995 6.905952995
-6.905952995 -3.452976497 6.905952995
```

length of vectors

```
10.358929492 9.766492386 10.358929492
```

position of ions in fractional coordinates

```
0.000000000 0.000000000 0.000000000
0.454545455 0.818181818 0.727272727
0.727272727 0.409090909 0.363636364
0.727272727 0.909090909 0.363636364
0.181818182 0.227272727 0.090909091
0.909090909 0.636363636 0.454545455
0.090909091 0.863636364 0.545454545
0.363636364 0.454545455 0.181818182
0.818181818 0.272727273 0.909090909
0.272727273 0.090909091 0.636363636
0.545454545 0.681818182 0.272727273
0.363636364 0.954545455 0.181818182
0.000000000 0.500000000 0.000000000
0.454545455 0.318181818 0.727272727
0.181818182 0.727272727 0.090909091
0.636363636 0.545454545 0.818181818
0.909090909 0.136363636 0.454545455
0.090909091 0.363636364 0.545454545
0.818181818 0.772727273 0.909090909
```

0.272727273	0.590909091	0.636363636
0.545454545	0.181818182	0.272727273
0.636363636	0.045454545	0.818181818
0.136363636	0.295454545	0.818181818
0.590909091	0.113636364	0.545454545
0.863636364	0.704545455	0.181818182
0.863636364	0.204545455	0.181818182
0.318181818	0.522727273	0.909090909
0.045454545	0.931818182	0.272727273
0.227272727	0.159090909	0.363636364
0.500000000	0.750000000	0.000000000
0.954545455	0.568181818	0.727272727
0.409090909	0.386363636	0.454545455
0.681818182	0.977272727	0.090909091
0.500000000	0.250000000	0.000000000
0.136363636	0.795454545	0.818181818
0.590909091	0.613636364	0.545454545
0.318181818	0.022727273	0.909090909
0.772727273	0.840909091	0.636363636
0.045454545	0.431818182	0.272727273
0.227272727	0.659090909	0.363636364
0.954545455	0.068181818	0.727272727
0.409090909	0.886363636	0.454545455
0.681818182	0.477272727	0.090909091
0.772727273	0.340909091	0.636363636

68 atoms

volume of cell : 1399.7800

lattice vectors of the cell

10.358929492	3.452976497	3.452976497
0.000000000	6.905952995	10.358929492
3.452976497	-10.358929492	3.452976497

length of vectors

11.452227451	12.449883814	11.452227451
--------------	--------------	--------------

position of ions in fractional coordinates

0.000000000	0.000000000	0.000000000
0.176470588	0.117647059	0.470588235
0.352941176	0.235294118	0.941176471
0.029411765	0.352941176	0.911764706
0.852941176	0.235294118	0.441176471
0.529411765	0.352941176	0.411764706
0.705882353	0.470588235	0.882352941
0.205882353	0.470588235	0.382352941
0.382352941	0.588235294	0.852941176
0.058823529	0.705882353	0.823529412
0.882352941	0.588235294	0.352941176
0.558823529	0.705882353	0.323529412
0.735294118	0.823529412	0.794117647
0.235294118	0.823529412	0.294117647
0.411764706	0.941176471	0.764705882
0.088235294	0.058823529	0.735294118
0.911764706	0.941176471	0.264705882
0.588235294	0.058823529	0.235294118
0.764705882	0.176470588	0.705882353
0.264705882	0.176470588	0.205882353
0.441176471	0.294117647	0.676470588
0.117647059	0.411764706	0.647058824
0.941176471	0.294117647	0.176470588
0.617647059	0.411764706	0.147058824
0.794117647	0.529411765	0.617647059
0.294117647	0.529411765	0.117647059
0.470588235	0.647058824	0.588235294
0.147058824	0.764705882	0.558823529
0.970588235	0.647058824	0.088235294
0.647058824	0.764705882	0.058823529
0.823529412	0.882352941	0.529411765
0.323529412	0.882352941	0.029411765
0.500000000	0.000000000	0.500000000
0.676470588	0.117647059	0.970588235
0.176470588	0.117647059	0.970588235
0.352941176	0.235294118	0.441176471

```

0.529411765 0.352941176 0.911764706
0.205882353 0.470588235 0.882352941
0.029411765 0.352941176 0.411764706
0.705882353 0.470588235 0.382352941
0.882352941 0.588235294 0.852941176
0.382352941 0.588235294 0.352941176
0.558823529 0.705882353 0.823529412
0.235294118 0.823529412 0.794117647
0.058823529 0.705882353 0.323529412
0.735294118 0.823529412 0.294117647
0.911764706 0.941176471 0.764705882
0.411764706 0.941176471 0.264705882
0.588235294 0.058823529 0.735294118
0.264705882 0.176470588 0.705882353
0.088235294 0.058823529 0.235294118
0.764705882 0.176470588 0.205882353
0.941176471 0.294117647 0.676470588
0.441176471 0.294117647 0.176470588
0.617647059 0.411764706 0.647058824
0.294117647 0.529411765 0.617647059
0.117647059 0.411764706 0.147058824
0.794117647 0.529411765 0.117647059
0.970588235 0.647058824 0.588235294
0.470588235 0.647058824 0.088235294
0.647058824 0.764705882 0.558823529
0.323529412 0.882352941 0.529411765
0.147058824 0.764705882 0.058823529
0.823529412 0.882352941 0.029411765
0.000000000 0.000000000 0.500000000
0.500000000 0.000000000 0.000000000
0.676470588 0.117647059 0.470588235
0.852941176 0.235294118 0.941176471

```

128 atoms

volume of cell : 2634.8800

lattice vectors of the cell

```

13.811905989 0.000000000 0.000000000
0.000000000 13.811905989 0.000000000
0.000000000 0.000000000 13.811905989

```

length of vectors

```

13.811905989 13.811905989 13.811905989

```

position of ions in fractional coordinates

```

0.000000000 0.000000000 0.000000000
0.000000000 0.000000000 0.250000000
0.000000000 0.000000000 0.500000000
0.000000000 0.000000000 0.750000000
0.000000000 0.250000000 0.000000000
0.000000000 0.250000000 0.250000000
0.000000000 0.250000000 0.500000000
0.000000000 0.250000000 0.750000000
0.000000000 0.500000000 0.000000000
0.000000000 0.500000000 0.250000000
0.000000000 0.500000000 0.500000000
0.000000000 0.500000000 0.750000000
0.000000000 0.750000000 0.000000000
0.000000000 0.750000000 0.250000000
0.000000000 0.750000000 0.500000000
0.000000000 0.750000000 0.750000000
0.250000000 0.000000000 0.000000000
0.250000000 0.000000000 0.250000000
0.250000000 0.000000000 0.500000000
0.250000000 0.000000000 0.750000000
0.250000000 0.250000000 0.000000000
0.250000000 0.250000000 0.250000000
0.250000000 0.250000000 0.500000000
0.250000000 0.250000000 0.750000000
0.250000000 0.500000000 0.000000000
0.250000000 0.500000000 0.250000000
0.250000000 0.500000000 0.500000000
0.250000000 0.500000000 0.750000000
0.250000000 0.750000000 0.000000000

```



```

0.625000000 0.625000000 0.625000000
0.625000000 0.625000000 0.875000000
0.625000000 0.875000000 0.125000000
0.625000000 0.875000000 0.375000000
0.625000000 0.875000000 0.625000000
0.625000000 0.875000000 0.875000000
0.875000000 0.125000000 0.125000000
0.875000000 0.125000000 0.375000000
0.875000000 0.125000000 0.625000000
0.875000000 0.125000000 0.875000000
0.875000000 0.375000000 0.125000000
0.875000000 0.375000000 0.375000000
0.875000000 0.375000000 0.625000000
0.875000000 0.375000000 0.875000000
0.875000000 0.625000000 0.125000000
0.875000000 0.625000000 0.375000000
0.875000000 0.625000000 0.625000000
0.875000000 0.625000000 0.875000000
0.875000000 0.875000000 0.125000000
0.875000000 0.875000000 0.375000000
0.875000000 0.875000000 0.625000000
0.875000000 0.875000000 0.875000000

```

208 atoms

volume of cell : 4281.6800

lattice vectors of the cell

```

13.811905989 -6.905952995 6.905952995
0.000000000 13.811905989 6.905952995
-6.905952995 -6.905952995 13.811905989

```

length of vectors

```

16.916061024 15.442180345 16.916061024

```

position of ions in fractional coordinates

```

0.000000000 0.000000000 0.000000000
0.923076923 0.384615385 0.846153846
0.615384615 0.923076923 0.230769231
0.461538462 0.692307692 0.923076923
0.846153846 0.769230769 0.692307692
0.153846154 0.230769231 0.307692308
0.538461538 0.307692308 0.076923077
0.230769231 0.846153846 0.461538462
0.384615385 0.076923077 0.769230769
0.769230769 0.153846154 0.538461538
0.076923077 0.615384615 0.153846154
0.307692308 0.461538462 0.615384615
0.692307692 0.538461538 0.384615385
0.076923077 0.115384615 0.153846154
0.000000000 0.500000000 0.000000000
0.692307692 0.038461538 0.384615385
0.538461538 0.807692308 0.076923077
0.923076923 0.884615385 0.846153846
0.230769231 0.346153846 0.461538462
0.615384615 0.423076923 0.230769231
0.307692308 0.961538462 0.615384615
0.461538462 0.192307692 0.923076923
0.846153846 0.269230769 0.692307692
0.153846154 0.730769231 0.307692308
0.384615385 0.576923077 0.769230769
0.769230769 0.653846154 0.538461538
0.961538462 0.192307692 0.923076923
0.884615385 0.576923077 0.769230769
0.576923077 0.115384615 0.153846154
0.423076923 0.884615385 0.846153846
0.807692308 0.961538462 0.615384615
0.115384615 0.423076923 0.230769231
0.500000000 0.500000000 0.000000000
0.192307692 0.038461538 0.384615385
0.346153846 0.269230769 0.692307692
0.730769231 0.346153846 0.461538462
0.038461538 0.807692308 0.076923077
0.269230769 0.653846154 0.538461538
0.653846154 0.730769231 0.307692308

```

0.038461538	0.307692308	0.076923077
0.961538462	0.692307692	0.923076923
0.653846154	0.230769231	0.307692308
0.500000000	0.000000000	0.000000000
0.884615385	0.076923077	0.769230769
0.192307692	0.538461538	0.384615385
0.576923077	0.615384615	0.153846154
0.269230769	0.153846154	0.538461538
0.423076923	0.384615385	0.846153846
0.807692308	0.461538462	0.615384615
0.115384615	0.923076923	0.230769231
0.346153846	0.769230769	0.692307692
0.730769231	0.846153846	0.461538462
0.192307692	0.038461538	0.884615385
0.115384615	0.423076923	0.730769231
0.807692308	0.961538462	0.115384615
0.653846154	0.730769231	0.807692308
0.038461538	0.807692308	0.576923077
0.346153846	0.269230769	0.192307692
0.730769231	0.346153846	0.961538462
0.423076923	0.884615385	0.346153846
0.576923077	0.115384615	0.653846154
0.961538462	0.192307692	0.423076923
0.269230769	0.653846154	0.038461538
0.500000000	0.500000000	0.500000000
0.884615385	0.576923077	0.269230769
0.269230769	0.153846154	0.038461538
0.192307692	0.538461538	0.884615385
0.884615385	0.076923077	0.269230769
0.730769231	0.846153846	0.961538462
0.115384615	0.923076923	0.730769231
0.423076923	0.384615385	0.346153846
0.807692308	0.461538462	0.115384615
0.500000000	0.000000000	0.500000000
0.653846154	0.230769231	0.807692308
0.038461538	0.307692308	0.576923077
0.346153846	0.769230769	0.192307692
0.576923077	0.615384615	0.653846154
0.961538462	0.692307692	0.423076923
0.153846154	0.230769231	0.807692308
0.076923077	0.615384615	0.653846154
0.769230769	0.153846154	0.038461538
0.615384615	0.923076923	0.730769231
0.000000000	0.000000000	0.500000000
0.307692308	0.461538462	0.115384615
0.692307692	0.538461538	0.884615385
0.384615385	0.076923077	0.269230769
0.538461538	0.307692308	0.576923077
0.923076923	0.384615385	0.346153846
0.230769231	0.846153846	0.961538462
0.461538462	0.692307692	0.423076923
0.846153846	0.769230769	0.192307692
0.230769231	0.346153846	0.961538462
0.153846154	0.730769231	0.807692308
0.846153846	0.269230769	0.192307692
0.692307692	0.038461538	0.884615385
0.076923077	0.115384615	0.653846154
0.384615385	0.576923077	0.269230769
0.769230769	0.653846154	0.038461538
0.461538462	0.192307692	0.423076923
0.615384615	0.423076923	0.730769231
0.000000000	0.500000000	0.500000000
0.307692308	0.961538462	0.115384615
0.538461538	0.807692308	0.576923077
0.923076923	0.884615385	0.346153846
0.115384615	0.173076923	0.980769231
0.038461538	0.557692308	0.826923077
0.730769231	0.096153846	0.211538462
0.576923077	0.865384615	0.903846154
0.961538462	0.942307692	0.673076923
0.269230769	0.403846154	0.288461538
0.653846154	0.480769231	0.057692308
0.346153846	0.019230769	0.442307692
0.500000000	0.250000000	0.750000000
0.884615385	0.326923077	0.519230769
0.192307692	0.788461538	0.134615385
0.423076923	0.634615385	0.596153846

0.807692308	0.711538462	0.365384615
0.192307692	0.288461538	0.134615385
0.115384615	0.673076923	0.980769231
0.807692308	0.211538462	0.365384615
0.653846154	0.980769231	0.057692308
0.038461538	0.057692308	0.826923077
0.346153846	0.519230769	0.442307692
0.730769231	0.596153846	0.211538462
0.423076923	0.134615385	0.596153846
0.576923077	0.365384615	0.903846154
0.961538462	0.442307692	0.673076923
0.269230769	0.903846154	0.288461538
0.500000000	0.750000000	0.750000000
0.884615385	0.826923077	0.519230769
0.076923077	0.365384615	0.903846154
0.000000000	0.750000000	0.750000000
0.692307692	0.288461538	0.134615385
0.538461538	0.057692308	0.826923077
0.923076923	0.134615385	0.596153846
0.230769231	0.596153846	0.211538462
0.615384615	0.673076923	0.980769231
0.307692308	0.211538462	0.365384615
0.461538462	0.442307692	0.673076923
0.846153846	0.519230769	0.442307692
0.153846154	0.980769231	0.057692308
0.384615385	0.826923077	0.519230769
0.769230769	0.903846154	0.288461538
0.153846154	0.480769231	0.057692308
0.076923077	0.865384615	0.903846154
0.769230769	0.403846154	0.288461538
0.615384615	0.173076923	0.980769231
0.000000000	0.250000000	0.750000000
0.307692308	0.711538462	0.365384615
0.692307692	0.788461538	0.134615385
0.384615385	0.326923077	0.519230769
0.538461538	0.557692308	0.826923077
0.923076923	0.634615385	0.596153846
0.230769231	0.096153846	0.211538462
0.461538462	0.942307692	0.673076923
0.846153846	0.019230769	0.442307692
0.307692308	0.211538462	0.865384615
0.230769231	0.596153846	0.711538462
0.923076923	0.134615385	0.096153846
0.769230769	0.903846154	0.788461538
0.153846154	0.980769231	0.557692308
0.461538462	0.442307692	0.173076923
0.846153846	0.519230769	0.942307692
0.538461538	0.057692308	0.326923077
0.692307692	0.288461538	0.634615385
0.076923077	0.365384615	0.403846154
0.384615385	0.826923077	0.019230769
0.615384615	0.673076923	0.480769231
0.000000000	0.750000000	0.250000000
0.384615385	0.326923077	0.019230769
0.307692308	0.711538462	0.865384615
0.000000000	0.250000000	0.250000000
0.846153846	0.019230769	0.942307692
0.230769231	0.096153846	0.711538462
0.538461538	0.557692308	0.326923077
0.923076923	0.634615385	0.096153846
0.615384615	0.173076923	0.480769231
0.769230769	0.403846154	0.788461538
0.153846154	0.480769231	0.557692308
0.461538462	0.942307692	0.173076923
0.692307692	0.788461538	0.634615385
0.076923077	0.865384615	0.403846154
0.269230769	0.403846154	0.788461538
0.192307692	0.788461538	0.634615385
0.884615385	0.326923077	0.019230769
0.730769231	0.096153846	0.711538462
0.115384615	0.173076923	0.480769231
0.423076923	0.634615385	0.096153846
0.807692308	0.711538462	0.865384615
0.500000000	0.250000000	0.250000000
0.653846154	0.480769231	0.557692308
0.038461538	0.557692308	0.326923077
0.346153846	0.019230769	0.942307692

0.576923077	0.865384615	0.403846154
0.961538462	0.942307692	0.173076923
0.346153846	0.519230769	0.942307692
0.269230769	0.903846154	0.788461538
0.961538462	0.442307692	0.173076923
0.807692308	0.211538462	0.865384615
0.192307692	0.288461538	0.634615385
0.500000000	0.750000000	0.250000000
0.884615385	0.826923077	0.019230769
0.576923077	0.365384615	0.403846154
0.730769231	0.596153846	0.711538462
0.115384615	0.673076923	0.480769231
0.423076923	0.134615385	0.096153846
0.653846154	0.980769231	0.557692308
0.038461538	0.057692308	0.326923077

* andreas.grueneis@tuwien.ac.at

- [1] G. Knizia, T. B. Adler, and H.-J. Werner, *The Journal of Chemical Physics* **130**, 054104 (2009), <https://doi.org/10.1063/1.3054300>.
- [2] M. Valiev, E. Bylaska, N. Govind, K. Kowalski, T. Straatsma, H. Van Dam, D. Wang, J. Nieplocha, E. Apra, T. Windus, and W. de Jong, *Comput. Phys. Commun.* **181**, 1477 (2010).
- [3] “cc4s; available from <https://manuals.cc4s.org>.” .
- [4] A. Gallo, F. Hummel, A. Irmeler, and A. Grüneis, *J. Chem. Phys.* **154**, 064106 (2021).
- [5] A. Irmeler, A. Gallo, and A. Grüneis, *The Journal of Chemical Physics* **154**, 234103 (2021), <https://doi.org/10.1063/5.0050054>.
- [6] S. Hirata, I. Grabowski, M. Tobita, and R. J. Bartlett, *Chemical Physics Letters* **345**, 475 (2001).
- [7] G. Kresse and J. Furthmüller, *Phys. Rev. B* **54**, 11169 (1996).
- [8] G. Kresse and D. Joubert, *Phys. Rev. B* **59**, 1758 (1999).
- [9] A. Grüneis, G. H. Booth, M. Marsman, J. Spencer, A. Alavi, and G. Kresse, *J. Chem. Theory Comput.* **7**, 2780 (2011).
- [10] F. Hummel, T. Tsatsoulis, and A. Grüneis, *J. Chem. Phys.* **146**, 124105 (2017).